PROCEEDINGS OF SCIENCE

Lattice-based Equation of State of QCD matter with a critical point

Claudia Ratti*
Department of Physics, University of Houston
E-mail: cratti@uh.edu

We build a family of Equations of State (EoS) for QCD, which match the lattice QCD results up to $\mathcal{O}(\mu_B^4)$, and contain a critical point in the 3D Ising model universality class. We place the critical point in the chemical potential range covered by the second Beam Energy Scan (BESII) at the Relativistic Heavy Ion Collider (RHIC). We show the effect of the critical point on several thermodynamic observables and discuss possible constraints on the parameters, which arise from mapping the Ising model phase diagram onto the QCD one.

Corfu Summer Institute 2018 "School and Workshops on Elementary Particle Physics and Gravity" (CORFU2018)
31 August - 28 September, 2018
Corfu, Greece

*Speaker.

PoS(CORFU2018)161

1. Introduction

The main purpose of the second Beam Energy Scan at RHIC is to discover the critical point on the QCD phase diagram, which separates the known crossover transition at low chemical potential μ_B [1] from a postulated first order phase transition at larger density/chemical potential. A first principle prediction of the existence and location of the critical point is still missing, due to the fermionic sign problem that hinders Monte Carlo simulations at finite chemical potentials. However, the existence of the critical point has been predicted by several QCD-like models (for a review see e.g. [2]). The location of the critical point depends on the model used to predict it, which makes its experimental search very challenging. In view of the BESII, it is therefore important to predict the behavior of experimental observables in the vicinity of the critical point.

Hydrodynamical simulations have proven to be extremely successful in describing the matter created in heavy-ion collisions. Even if hydrodynamics itself needs to be modified in the vicinity of a critical point [3, 4, 5, 6], the equation of state which serves as an input to these simulations must contain a critical point with the correct singular behavior, besides reproducing all known constraints from lattice QCD. We have recently constructed a family of equations of state, which match lattice QCD results up to $\mathcal{O}(\mu_B^4)$ and contain a critical point in the 3D Ising model universality class [7].

At $\mu_B = 0$, the EoS of QCD is known with high precision, in the case of 2+1 [8, 9, 10] and 2+1+1 [11] quark flavors. Lattice QCD simulations allow us to reconstruct the equation of state as a Taylor series in powers of μ_B/T [12, 13, 14, 15, 16] or an analytic continuation from imaginary μ_B [17, 18, 19, 20, 21, 22, 23, 24]. The Taylor expansion of the pressure in μ_B/T around $\mu_B = 0$ can be written as:

$$P(T,\mu_B) = T^4 \sum_n c_{2n}(T) \left(\frac{\mu_B}{T}\right)^{2n} , \tag{1.1}$$

where the coefficients of the expansion are the susceptibilities of the baryon number:

$$c_n(T) = \frac{1}{n!} \frac{\partial^n P/T^4}{\partial(\mu_B/T)^n}\bigg|_{\mu_B=0} = \frac{1}{n!}\chi_n(T) . \tag{1.2}$$

After the early results for c_2, c_4 and c_6 [13], the first continuum extrapolated results for c_2 were published in Ref. [25]; in Ref. [26] c_4 was shown, but only at finite lattice spacing. The continuum limit for c_6 was published for the first time in [27], and later in [28]. In [29], a first determination of c_8, at two values of the temperature and $N_t = 8$ was presented. More recently, an estimate of the temperature dependence of c_8 was presented at $N_t = 12$ [30]. The advantage of the Taylor expansion method is that all the quantities are calculated at vanishing baryon chemical potential, where lattice QCD simulations do not suffer from the fermion sign problem (for a recent review, see e.g. [31]).

2. Ising model Equation of State

The parameterization of the scaling Equation of state for the Ising model is usually given in terms of magnetization M as a function of magnetic field h and reduced temperature $r = (T - T_c)/T_c$ (or auxiliary variables R and θ. The following form for the parametrization meets the requirements

[32, 33, 34, 35]:

$$M = M_0 R^\beta \theta \,, \tag{2.1}$$

$$h = h_0 R^{\beta\delta} \tilde{h}(\theta) \,, \tag{2.2}$$

$$r = R(1-\theta^2) \,. \tag{2.3}$$

where M_0, h_0 are normalization constants, $\tilde{h}(\theta) = \theta(1+a\theta^2+b\theta^4)$ with $a = -0.76201$, $b = 0.00804$. $\beta \simeq 0.326$ and $\delta \simeq 4.80$ are 3D Ising critical exponents, and the parameters take on the values $R \geq 0$, $|\theta| \leq \theta_0 \simeq 1.154$, θ_0 being the first non-trivial zero of $\tilde{h}(\theta)$. The values of the normalization constants are such that $M(r=-1, h=0^+) = 1$ and $M(r=0,h) \propto \mathrm{sgn}(h)\,|h|^{1/\delta}$: this yields $M_0 \simeq 0.605$, $h_0 \simeq 0.394$.

The Gibbs free energy density then follows from this parametrization:

$$G(h,r) = F(M,r) - Mh \,, \tag{2.4}$$

where $F(M,r)$ is the free energy density, defined as:

$$F(M,h) = h_0 M_0 R^{2-\alpha} g(\theta) \,, \tag{2.5}$$

where $\alpha \simeq 0.11$ is another critical exponent of the 3D Ising model (also, the relation $2-\alpha = \beta(\delta+1)$ holds). The function $g(\theta)$ is fixed by noticing that $h = (\partial F/\partial M)_h$ and solving the following differential equation:

$$\tilde{h}(\theta)(1-\theta^2+2\beta\theta^2) = 2(2-\alpha)\theta g(\theta) + (1-\theta^2) g'(\theta) \tag{2.6}$$

which results in:

$$g(\theta) = c_0 + c_1(1-\theta^2) + c_2(1-\theta^2)^2 + c_3(1-\theta^2)^3 \,, \tag{2.7}$$

with:

$$c_0 = \frac{\beta}{2-\alpha}(1+a+b) \,, \tag{2.8}$$

$$c_1 = -\frac{1}{2}\frac{1}{\alpha-1}\left\{(1-2\beta)(1+a+b) - 2\beta(a+2b)\right\} \,, \tag{2.9}$$

$$c_2 = -\frac{1}{2\alpha}\left\{2\beta b - (1-2\beta)(a+2b)\right\} \,, \tag{2.10}$$

$$c_3 = -\frac{1}{2(\alpha+1)} b(1-2\beta) \,. \tag{2.11}$$

To proceed with the mapping of the Ising model onto the QCD phase diagram we notice that the Gibbs free energy density equals the pressure up to a minus sign: $G = -P$, hence:

$$P_{\mathrm{Ising}}(R,\theta) = h_0 M_0 R^{2-\alpha}\left[\theta\tilde{h}(\theta) - g(\theta)\right] \,. \tag{2.12}$$

We now map the phase diagram of the 3D Ising model onto the one of QCD, so that the critical point of the Ising model $r = h = 0$ corresponds to the one of QCD, and that the lines of first order phase transition and crossover in the Ising model are mapped onto those of QCD.

The simplest way to do so is through a linear map as follows [36]:

$$\frac{T-T_C}{T_C} = w\left(r\rho\,\sin\alpha_1 + h\,\sin\alpha_2\right)\,, \tag{2.13}$$

$$\frac{\mu_B-\mu_{BC}}{T_C} = w\left(-r\rho\,\cos\alpha_1 - h\,\cos\alpha_2\right)\,, \tag{2.14}$$

which can be visualized in Fig. 1. This map makes use of six parameters, two of which correspond to the location of the critical point on the QCD phase diagram, two are the angles that the r and h axes form with the $T=$ const. lines, and (w,ρ) are scale factors for the variables r and h. While w represents a *global* scaling for the Ising variables, namely determining the size of the critical region, ρ represents a *relative* scaling of r and h, thus roughly determining the shape of it.

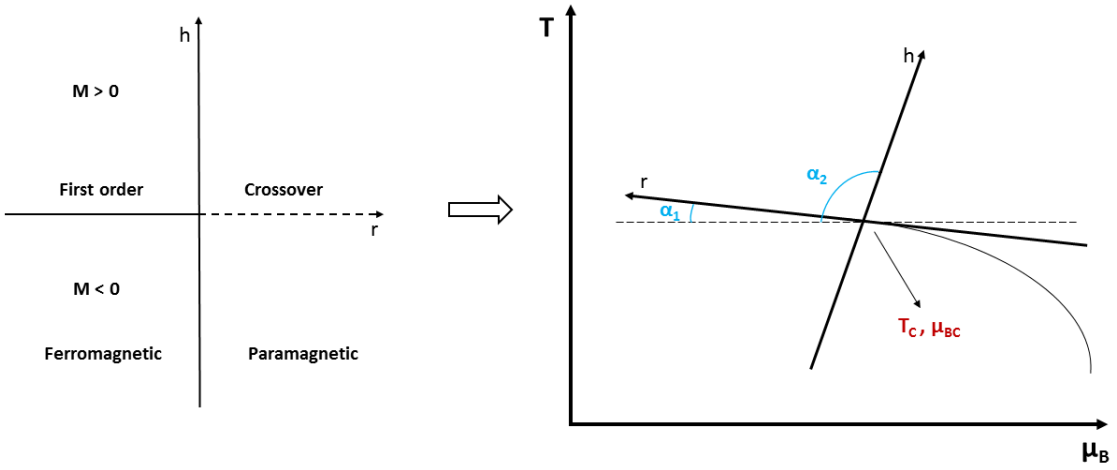

Figure 1: Non-universal map from Ising variables (r,h) to QCD coordinates (T,μ_B)

At this point it is possible to transport the thermodynamics of the Ising model (written in terms of (R,θ)), into the QCD phase diagram, given a choice of parameters for the map.

It is possible to impose some constraint on the parameter choice by making use of additional arguments for the location of the critical point. For example, the curvature of the transition line at $\mu_B=0$ has been estimated in lattice simulations [37, 38, 39]. The shape of such transition line can be approximated with a parabola:

$$T = T_0 + \kappa T_0\left(\frac{\mu_B}{T_0}\right)^2 + \mathcal{O}(\mu_B^4) \tag{2.15}$$

where T_0 and κ are the transition temperature and curvature of the transition line at $\mu_B=0$, respectively. The number of the parameters is thus reduced to four, the angle α_1 also being fixed by:

$$\alpha_1 = \tan^{-1}\left(2\frac{\kappa}{T_0}\mu_{BC}\right)\,. \tag{2.16}$$

In the following, remembering that the aim of the EoS is to be employed in hydrodynamic simulations for heavy-ion collisions in the BES-II program, we will consider a choice of the baryonic

chemical potential which is $\mu_{BC} = 350$ MeV, resulting in:

$$T_C \simeq 143.2\,\text{MeV}\,, \qquad \alpha_1 \simeq 3.85^\circ\,. \tag{2.17}$$

In addition, the axes are chosen to be orthogonal, as we already mentioned, so that $\alpha_2 \simeq 93.85^\circ$. Finally, the scaling parameters are initially chosen as:

$$w = 1\,, \qquad \rho = 2\,. \tag{2.18}$$

Later we will explore different choices for w and ρ, trying to reduce their acceptable range on the basis of physical conditions for the thermodynamic quantities.

3. Thermodynamics

In the following, we assume that the lattice QCD expansion coefficients can be written as a sum of an "Ising" contribution coming from the critical point of QCD, and a "Non-Ising" contribution, which would contain the regular part as well as any other possible criticality present in the region of interest:

$$T^4 c_n^{\text{LAT}}(T) = T^4 c_n^{\text{Non-Ising}}(T) + f(T,\mu_B=0) c_n^{\text{Ising}}(T)\,. \tag{3.1}$$

where $f(T,\mu_B)$ is a regular function of the temperature and chemical potential, with dimension of energy to the fourth power. We choose $f(T,\mu_B) = T_C^4$. Note that Eq (3.1) is to be understood as a definition for the $c_n^{\text{Non-Ising}}$ coefficients, which we obtain as a difference between the other two contributions. The full pressure is then reconstructed simply by adding the critical contribution at any (T,μ_B) to the Taylor expanded "Non-Ising" one:

$$P(T,\mu_B) = T^4 \sum_n c_{2n}^{\text{Non-Ising}}(T) \left(\frac{\mu_B}{T}\right)^{2n} + P_{\text{crit}}^{\text{QCD}}(T,\mu_B)\,. \tag{3.2}$$

Note that in Eq. (3.2), the critical pressure is obtained from Eq. (2.12) with the multiplication by $f(T,\mu_B)$ in Eq. (3.1):

$$P_{\text{QCD}}^{\text{crit}}(T,\mu_B) = f(T,\mu_B) P^{\text{Ising}}(R(T,\mu_B),\theta(T,\mu_B))\,. \tag{3.3}$$

Because of the charge conjugation symmetry, in QCD the partition function needs to be an even function of the baryon chemical potential:

$$\mathscr{Z}(T,-\mu_B) = \mathscr{Z}(T,\mu_B)\,, \tag{3.4}$$

as well as the pressure. Thus QCD must possess a critical point at both μ_{BC} and $-\mu_{BC}$. To achieve this we need to write Eq. (3.5) below. This form does not modify the singular critical behavior at the critical point(s) and automatically ensures that the odd-power coefficients in the Taylor expansion in μ_B vanish, as they should.

$$\begin{aligned} P_{\text{QCD}}^{\text{crit}}(T,\mu_B) &= \frac{1}{2} f(T,\mu_B) P_{\text{symm}}^{\text{Ising}}(R(T,\mu_B),\theta(T,\mu_B)) = \\ &= \frac{1}{2} f(T,\mu_B) \left\{ P^{\text{Ising}}(R(T,\mu_B),\theta(T,\mu_B)) + P^{\text{Ising}}(R(T,-\mu_B),\theta(T,-\mu_B)) \right\}\,, \end{aligned} \tag{3.5}$$

which will have the effect of slightly changing the form of the critical pressure (the main one being that now the pressure at the critical point is non-zero, whereas it would be zero in the straightforward definition) but not its singular behavior, leaving all the even order derivatives unchanged.

In Fig.2 we can see the comparison between the lattice data (and the extension with the HRG model) and the resulting parametrization. The HRG model employed to calculate the pressure does not contain any interaction, and makes use of the most up to date particle list available from the Particle Data Group [40] (list PDG2016+ in [41]).

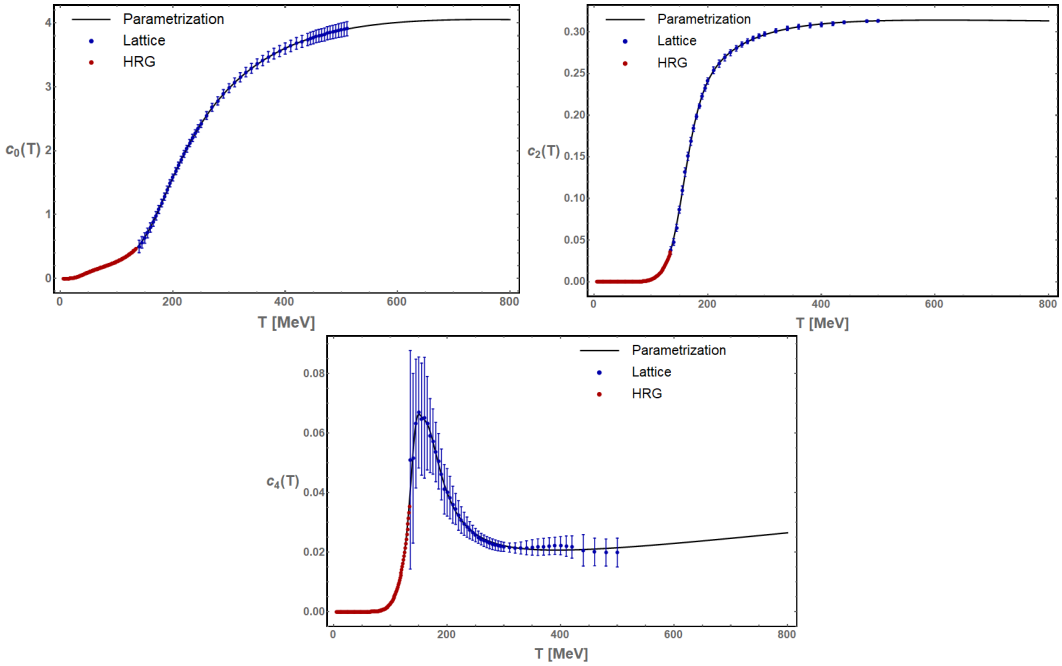

Figure 2: Parametrization of baryon susceptibilities from Lattice QCD [9, 42] and HRG model calculations.

Fig. 3 shows the comparison of the "Ising" and "Non-Ising" contributions to the parametrized lattice/HRG model results.

4. Results

To cure some pathological behavior of our EoS at small temperatures, we perform a smooth merging with the HRG model EoS.

The smooth merging can be obtained through a hyperbolic tangent as:

$$\frac{P_{\rm Final}(T,\mu_B)}{T^4} = \frac{P(T,\mu_B)}{T^4}\frac{1}{2}\left(1+\tanh\left(\frac{T-T'(\mu_B)}{\Delta T'}\right)\right)+ \\ +\frac{P_{\rm HRG}(T,\mu_B)}{T^4}\frac{1}{2}\left(1-\tanh\left(\frac{T-T'(\mu_B)}{\Delta T'}\right)\right), \tag{4.1}$$

where $T'(\mu_B)$ works as the "switching temperature", and $\Delta T'$ is roughly the size of the "overlap region" where both pressures contribute to the sum. The dependence on the baryon chemical potential of the "switching temperature" is chosen to be parabolic: this way, the "switching line"

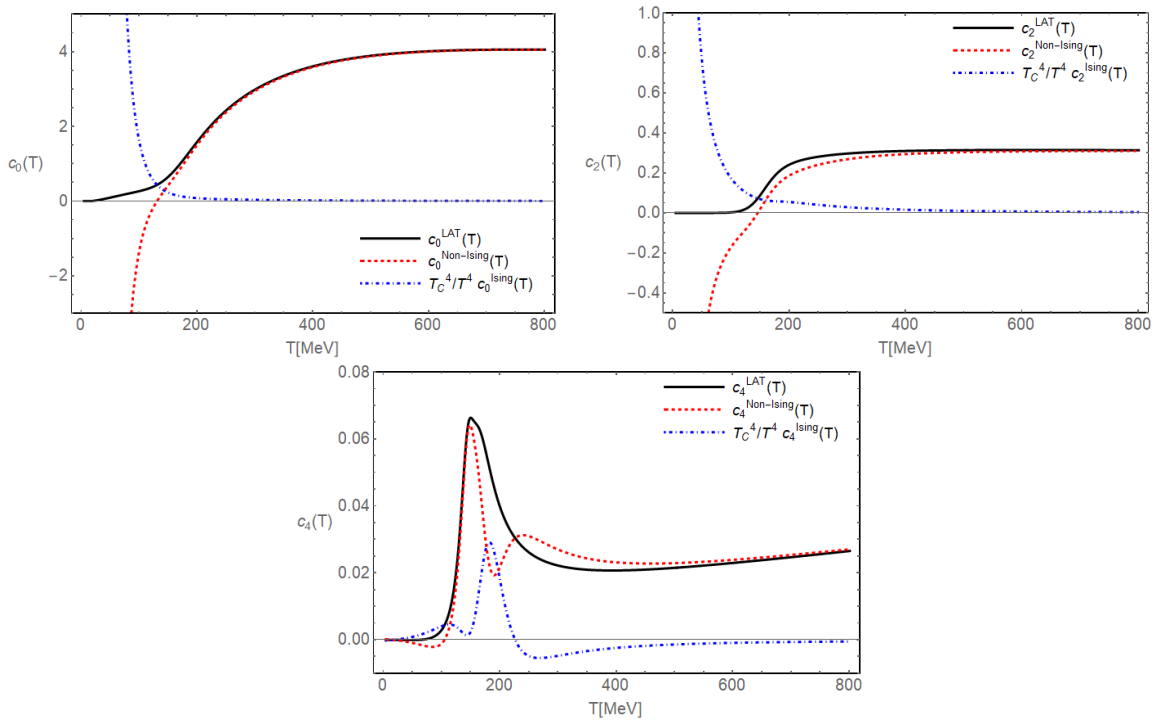

Figure 3: Comparison of critical (blue, dot-dashed) and "Non-Ising" (red, dashed) contributions to baryon susceptibilities up to $\mathcal{O}(\mu_B^4)$ with the parametrized lattice data (black, solid).

between the pressure from our procedure and the one from the HRG model is parallel to the chiral transition curve.

In order to complete the thermodynamic description of the finalized equation of state obtained in Eq. (4.1), we can compute various thermodynamic observables of interest. In addition to the pressure, we compute the entropy density, baryon density, energy density and speed of sound normalized by the correct power of the temperature:

$$\frac{P(T,\mu_B)}{T^4}\,, \qquad \frac{S(T,\mu_B)}{T^3} = \frac{1}{T^3}\left(\frac{\partial P}{\partial T}\right)_{\mu_B}\,, \frac{n_B(T,\mu_B)}{T^3} = \frac{1}{T^3}\left(\frac{\partial P}{\partial \mu_B}\right)_{T}\,, \tag{4.2}$$

$$\frac{\varepsilon(T,\mu_B)}{T^4} = \frac{S}{T^3} - \frac{P}{T^4} + \frac{\mu_B}{T}\frac{n_B}{T^3}\,, \qquad c_s^2(T,\mu_B) = \left(\frac{\partial P}{\partial \varepsilon}\right)_{S/n_B}\,. \tag{4.3}$$

They are shown in Figs. 4 - 8. The effect of the critical point on the thermodynamic isentropes (trajectories at constant S/n_B in the QCD phase diagram) is shown in Fig. 9. The effect of the critical point is clearly visible in the distortion of the isentropes at large chemical potentials. By requiring thermodynamic stability, i.e. positivity of pressure, entropy density, baryon density, energy density and speed of sound, and causality, i.e $c_s^2 < 1$, over the whole phase diagram, it is possible to reduce the range of acceptable parameters in the non-universal Ising $\mapsto$ QCD map. By keeping the location of the critical point fixed ($\mu_{BC} = 350\,\text{MeV}$, $T_C \simeq 143\,\text{MeV}$), as well as the orientation of the axes ($\alpha_1 \simeq 3.85^\circ$, $\alpha_2 - \alpha_1 = 90^\circ$), we investigated the role of the scaling parameters w, ρ. In Fig. 10, we can see in red the points corresponding to pathological parameter choices, while the blue dots correspond to acceptable ones. We notice that, while most commonly specific parameter

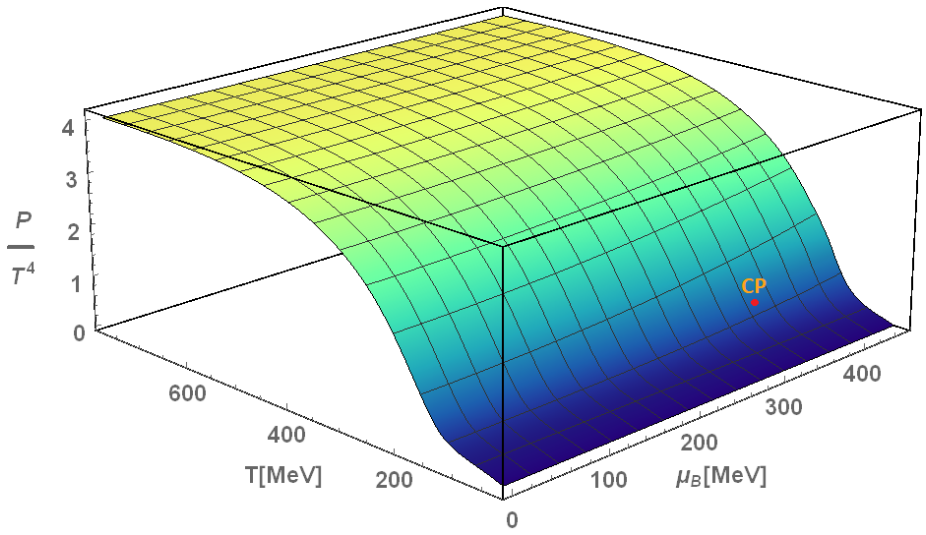

Figure 4: Pressure after merging with HRG.

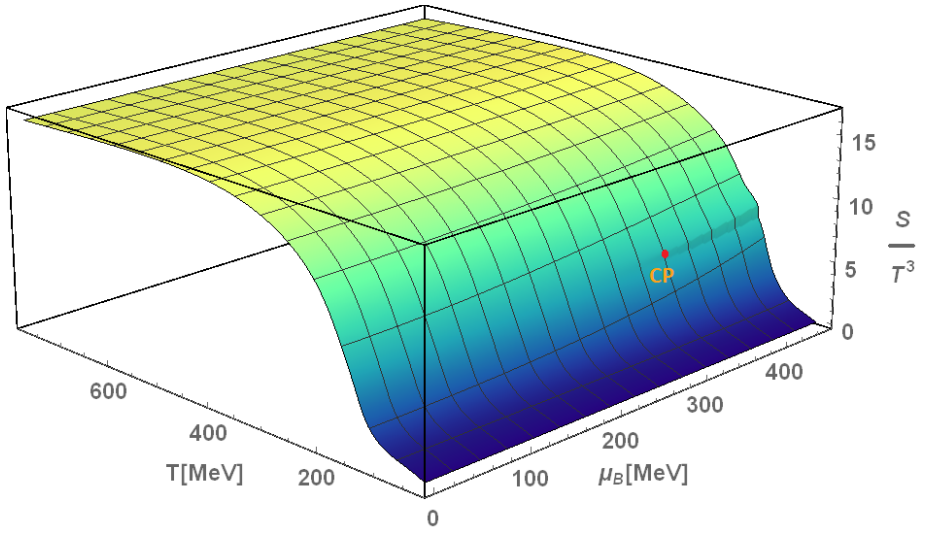

Figure 5: Entropy density after merging with HRG.

choices are unacceptable because of the negativity of n_B, for very low w ($w = 0.25$) we observe violation of causality as well ($c_s^2 > 1$).

5. Conclusions

We presented a family of equations of state, which match available lattice QCD results up to $O(\mu_B^4)$ and contain a critical point in the 3D Ising model universality class. These EoSs are meant to be used as an input into hydrodynamic simulations of the system created in heavy-ion collisions. A systematic scan of the parameter space, and relative comparison with experimental data from the BESII at RHIC, will hopefully allow us to constrain the size of the critical region and the location of the critical point.

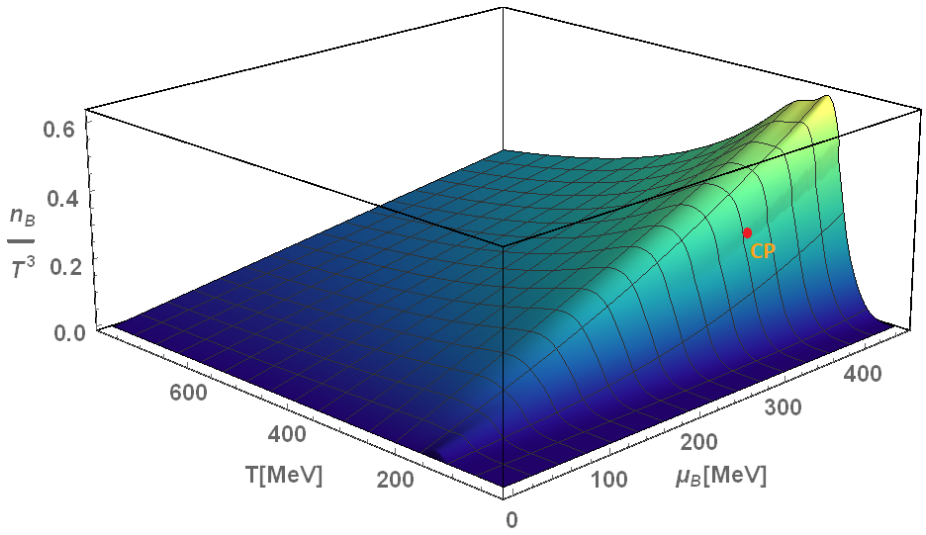

Figure 6: Baryon density after merging with HRG.

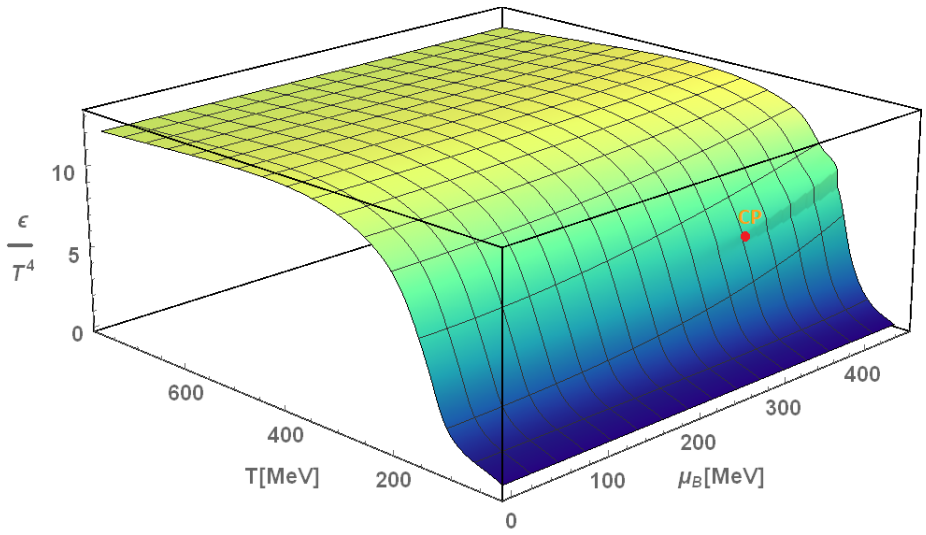

Figure 7: Energy density after merging with HRG.

Acknowledgements

This material is based upon work supported by the National Science Foundation under grant no. PHY-1654219 and by the U.S. Department of Energy, Office of Science, Office of Nuclear Physics within the framework of the Beam Energy Scan Theory (BEST) Topical Collaboration. The author also acknowledges the use of the Maxwell Cluster and the advanced support from the Center of Advanced Computing and Data Systems at the University of Houston.

References

[1] Aoki Y, Endrodi G, Fodor Z, Katz S D and Szabo K K 2006 *Nature* **443** 675–678 (*Preprint* `hep-lat/0611014`)

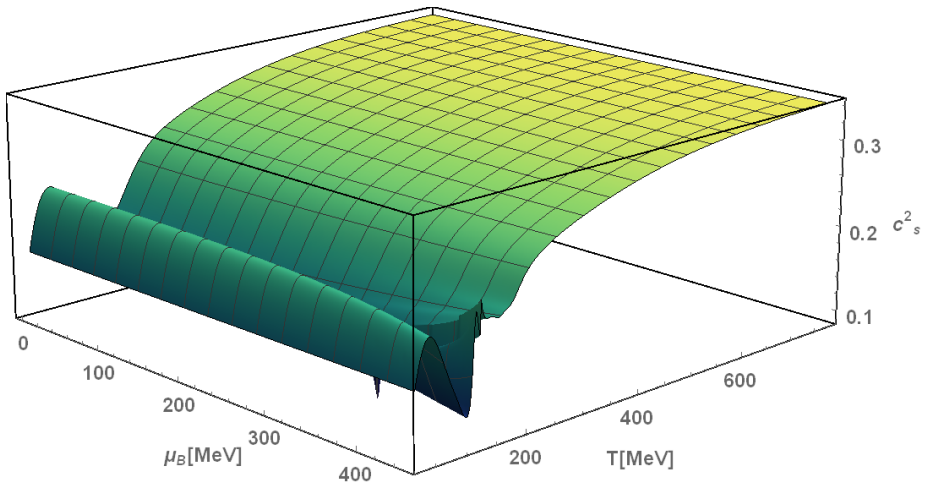

Figure 8: Speed of sound after merging with HRG.

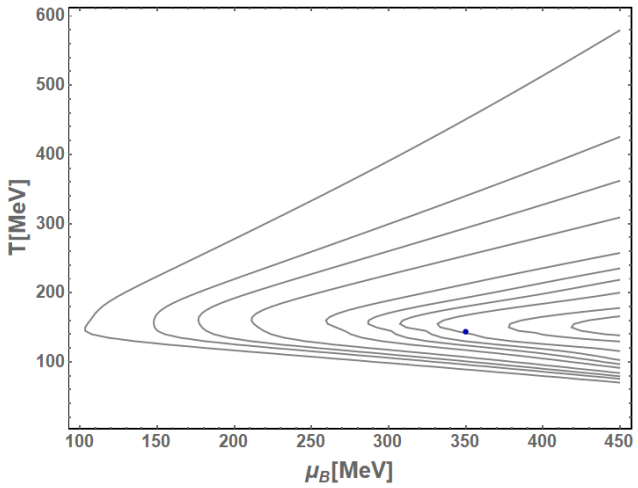

Figure 9: Lines of constant S/n_B (from left to right $S/n_B = 68, 50, 42, 35, 28, 25, 23, 21, 18, 16$) in the QCD phase diagram. The blue dot indicates the location of the critical point.

[2] Stephanov M A 2006 *PoS* **LAT2006** 024 (*Preprint* hep-lat/0701002)

[3] Stephanov M A 2010 *Phys. Rev.* **D81** 054012 (*Preprint* 0911.1772)

[4] Nahrgang M, Leupold S, Herold C and Bleicher M 2011 *Phys. Rev.* **C84** 024912 (*Preprint* 1105.0622)

[5] Stephanov M and Yin Y 2018 *Phys. Rev.* **D98** 036006 (*Preprint* 1712.10305)

[6] Nahrgang M, Bluhm M, Schäfer T and Bass S A 2018 (*Preprint* 1804.05728)

[7] Parotto P, Bluhm M, Mroczek D, Nahrgang M, Noronha-Hostler J, Rajagopal K, Ratti C, Schäfer T and Stephanov M 2018 (*Preprint* 1805.05249)

[8] Borsanyi S, Endrodi G, Fodor Z, Jakovac A, Katz S D, Krieg S, Ratti C and Szabo K K 2010 *JHEP* **11** 077 (*Preprint* 1007.2580)

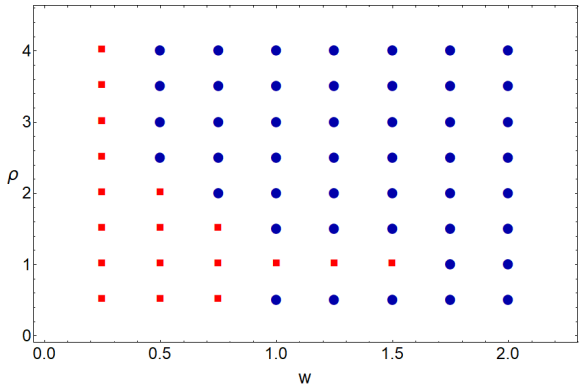

Figure 10: In red (squares) the points corresponding to pathological choices of parameters, in blue (dots) the acceptable ones.

[9] Borsanyi S, Fodor Z, Hoelbling C, Katz S D, Krieg S and Szabo K K 2014 *Phys. Lett.* **B730** 99–104 (*Preprint* 1309.5258)

[10] Bazavov A *et al.* (HotQCD) 2014 *Phys. Rev.* **D90** 094503 (*Preprint* 1407.6387)

[11] Borsanyi S *et al.* 2016 *Nature* **539** 69–71 (*Preprint* 1606.07494)

[12] Allton C R, Ejiri S, Hands S J, Kaczmarek O, Karsch F, Laermann E, Schmidt C and Scorzato L 2002 *Phys. Rev.* **D66** 074507 (*Preprint* hep-lat/0204010)

[13] Allton C R, Doring M, Ejiri S, Hands S J, Kaczmarek O, Karsch F, Laermann E and Redlich K 2005 *Phys. Rev.* **D71** 054508 (*Preprint* hep-lat/0501030)

[14] Gavai R V and Gupta S 2008 *Phys. Rev.* **D78** 114503 (*Preprint* 0806.2233)

[15] Basak S *et al.* (MILC) 2008 *PoS* **LATTICE2008** 171 (*Preprint* 0910.0276)

[16] Kaczmarek O, Karsch F, Laermann E, Miao C, Mukherjee S, Petreczky P, Schmidt C, Soeldner W and Unger W 2011 *Phys. Rev.* **D83** 014504 (*Preprint* 1011.3130)

[17] de Forcrand P and Philipsen O 2002 *Nucl. Phys.* **B642** 290–306 (*Preprint* hep-lat/0205016)

[18] D'Elia M and Lombardo M P 2003 *Phys. Rev.* **D67** 014505 (*Preprint* hep-lat/0209146)

[19] Wu L K, Luo X Q and Chen H S 2007 *Phys. Rev.* **D76** 034505 (*Preprint* hep-lat/0611035)

[20] D'Elia M, Di Renzo F and Lombardo M P 2007 *Phys. Rev.* **D76** 114509 (*Preprint* 0705.3814)

[21] Conradi S and D'Elia M 2007 *Phys. Rev.* **D76** 074501 (*Preprint* 0707.1987)

[22] de Forcrand P and Philipsen O 2008 *JHEP* **11** 012 (*Preprint* 0808.1096)

[23] D'Elia M and Sanfilippo F 2009 *Phys. Rev.* **D80** 014502 (*Preprint* 0904.1400)

[24] Moscicki J T, Wos M, Lamanna M, de Forcrand P and Philipsen O 2010 *Comput. Phys. Commun.* **181** 1715–1726 (*Preprint* 0911.5682)

[25] Borsanyi S, Endrodi G, Fodor Z, Katz S D, Krieg S, Ratti C and Szabo K K 2012 *JHEP* **08** 053 (*Preprint* 1204.6710)

[26] Hegde P (BNL-Bielefeld-CCNU) 2014 *Nucl. Phys.* **A931** 851–855 (*Preprint* 1408.6305)

[27] Gunther J, Bellwied R, Borsanyi S, Fodor Z, Katz S D, Pasztor A and Ratti C 2017 *EPJ Web Conf.* **137** 07008 (*Preprint* 1607.02493)

[28] Bazavov A *et al.* 2017 *Phys. Rev.* **D95** 054504 (*Preprint* 1701.04325)

[29] D'Elia M, Gagliardi G and Sanfilippo F 2017 *Phys. Rev.* **D95** 094503 (*Preprint* 1611.08285)

[30] Borsanyi S, Fodor Z, Guenther J N, Katz S K, Szabó K K, Pasztor A, Portillo I and Ratti C 2018 (*Preprint* 1805.04445)

[31] Ratti C 2018 *Rept. Prog. Phys.* **81** 084301 (*Preprint* 1804.07810)

[32] Nonaka C and Asakawa M 2005 *Phys. Rev.* **C71** 044904 (*Preprint* nucl-th/0410078)

[33] Guida R and Zinn-Justin J 1997 *Nucl. Phys.* **B489** 626–652 (*Preprint* hep-th/9610223)

[34] Schofield P, Litster J D and Ho J T 1969 *Phys. Rev. Lett.* **23** 1098–1102

[35] Bluhm M and Kampfer B 2006 *PoS* **CPOD2006** 004 (*Preprint* hep-ph/0611083)

[36] Rehr J J and Mermin N D 1973 *Phys. Rev.* **A8** 472–480

[37] Cea P, Cosmai L and Papa A 2016 *Phys. Rev.* **D93** 014507 (*Preprint* 1508.07599)

[38] Bonati C, D'Elia M, Mariti M, Mesiti M, Negro F and Sanfilippo F 2015 *Phys. Rev.* **D92** 054503 (*Preprint* 1507.03571)

[39] Bellwied R, Borsanyi S, Fodor Z, Günther J, Katz S D, Ratti C and Szabo K K 2015 *Phys. Lett.* **B751** 559–564 (*Preprint* 1507.07510)

[40] Patrignani C *et al.* (Particle Data Group) 2016 *Chin. Phys.* **C40** 100001

[41] Alba P *et al.* 2017 *Phys. Rev.* **D96** 034517 (*Preprint* 1702.01113)

[42] Bellwied R, Borsanyi S, Fodor Z, Katz S D, Pasztor A, Ratti C and Szabo K K 2015 *Phys. Rev.* **D92** 114505 (*Preprint* 1507.04627)